Available online at www.sciencedirect.com

ScienceDirect

Procedia CIRP 49 (2016) 33 – 38

www.elsevier.com/locate/procedia

The Second CIRP Conference on Biomanufacturing

Manufacture and characterisation of porous PLA scaffolds

Natacha Rodrigues [1], Matthew Benning[1], Ana M.Ferreira[1], Luke Dixon[2] and Kenny Dalgarno[1*]

[1]*School of Mechanical and Systems Engineering, Newcastle University, Newcastle, UK*

[2]*School of Chemistry, Newcastle University, Newcastle, UK*

* Kenny Dalgarno. Tel. 07871660860 . *E-mail address:* kenny.dalgarno@newcastle.ac.uk

Abstract

Bone scaffolds must have an appropriate porosity range with an interconnected and open porosity, and have a biodegradable rate and mechanical properties that match the injured tissue. The use of commercially available and low cost 3D printing machines offers the ability to fulfil these requirements. Therefore, one of the aims of this study was to manufacture a PLA scaffold by a two-step route: 1) 3D printing of a PLA porous bar and 2) laser cut PLA scaffolds from the 3D printed bar. Laser cutting did not cause any significant degradation issues and scanning electron microscopy showed that 3-D scaffolds had completely interconnected and uniform open porosity, with pore size between ~550 to 600 µm in both axial and transversal direction. Conversely, mechanical test of PLA scaffold indicated that both compressive modulus and stress at yield were decreased by the laser cutting step but they remained adequate for trabecular bone replacement. Finally, the in vitro degradation behaviour of PLA scaffolds after 8 weeks immersed in PBS, did not revealed any significant decrease of weight, molecular weight, and compressive properties.

Peer-review under responsibility of the scientific committee of The Second CIRP Conference on Biomanufacturing

Keywords: Bone;Scaffolds; Fused Filament Fabrication; Polylactic acid

1. Introduction

There are almost one million cases of skeletal defects a year which represents a major concern in both the USA and the EU because of associated socioeconomic problems [1]. Moreover these numbers are expected to increase due to worldwide life expectancy rises. Critical size bone defects cannot undergo self-healing, thus an intervention is required to restore normal operations. Autografts (bone harvested from the patient body) and allografts (bone harvested from a donor) are among the current procedures and are often associated with donor morbidity and disease transmission, respectively [2]. Tissue engineering (TE) has emerged as a promising intervention for the repair and regeneration of bone defects by overcoming the limitations of the standard procedures.

One of the most important approaches of the developing field of TE consists in the fabrication of a porous three-dimensional (3D) scaffold, which acts as a template for tissue regeneration, guiding cells to form functional and new tissue. Ideally a bone scaffold must be biocompatible, biodegradable, have the appropriate porosity range and interconnectivity, readily available and easy to manufacture [3-5]. Several groups have reported the importance of scaffold pore size in successful bone ingrowth [6]. Scaffolds with pores bigger than 300 µm were associated with greater penetration of mineralized tissue and cell migration towards the scaffold center, stimulating nutrient supply and waste products removal [7, 8]. Furthermore, a bone scaffold must provide mechanically functionality and stability allowing early post-operative function under physiologic loading conditions.

The use of Additive Manufacturing (AM) for tissue engineering has been growing in recent years by overcoming some limitations of conventional scaffold fabrication techniques [9]. For instance, fused filament fabrication (FFF) offers the ability to directly print 3D porous scaffolds with pre-designed shape, solvent-free, controlled pore size and interconnected porosity. Based on computer-aided design (CAD) models, 3D printers can easily fabricate a predesigned

Peer-review under responsibility of the scientific committee of The Second CIRP Conference on Biomanufacturing

doi:10.1016/j.procir.2015.07.025

patient specific tissue construct in a layer-by-layer fashion. Moreover, commercially available FFF machines can be considered a low cost system when compared to other AM techniques. However, one of the drawbacks of the FFF process is that fabricated 3D porous scaffolds are often characterised by closed edges instead of open porosity. At time of scaffold implantation, these closed edges can affect cell-biomaterial interaction by decreasing nutrients and waste products flow and affecting vascularization, which is essential for tissue growth. The current solution for achieving a structure with surrounding open pores involves cutting the edges of the fabricated scaffold [10].

Laser cutting can offer an effective, precise and fast solution for obtaining scaffolds with desired-shape and open porosity from a pre-fabricated 3D printed porous bar.

Therefore the aim of this study was to manufacture a scaffold by a two-step route: 1) 3D printing of a porous bar with a commercially available FFF machine and 2) laser cutting smaller scaffolds from the 3D printed bar.

Polylactic acid (PLA) was the material used to evaluate the approach. PLA is a recognized biomaterial, which can be processed using FFF. To determine the applicability of the fabricated scaffolds for bone tissue engineering, morphology and mechanical behaviour were assessed.

A key issue when choosing a material for temporary tissue engineering templates is its degradation rate. It is highly desirable to ensure that the degradation rate matches the speed of new tissue regeneration at the defect site. Therefore, a preliminary *in vitro* degradation study in PBS at 37°C of the fabricated PLA scaffolds was carried out.

2. Materials and Methods

2.1. Material

A polylactic acid 2.85-3.00mm filament (PLA, 4032D, Nature Works®) with an L-lactide: D-lactide ratio of 98:2 and a density of 1.24 g/cm^3 was the material used for the experimental work. The tensile modulus and elongation at break were 3784 MPa (D882) and 100% (D822), respectively, as reported by the manufacturer [11]. Commercially available PLA are in general copolymers of PLLA and poly (D,L-lactic acid) (PDLLA). PLA polymers with an L-lactide content more than ~ 90% tend to be crystalline while a lower amount results in amorphous PDLLA [12].

2.2. Scaffold fabrication

Fig.1 summarizes the scaffold fabrication route used during this study. The first step consisted in printing PLA rectangular porous bars with 32 x 86 x 5mm with a commercially available FFF machine (Ultimaker 2). Then discs with Ø10 mm were laser cut (LS3020, HPC Laser LTD) from the printed bars. The processing conditions used to cut the PLA rectangular porous plates were found to be to cut twice with a laser speed and power of 6.50 mm/s and 12 W, respectively.

The FFF printing process can be divided in 3 steps: A) design of the 3D model (CAD software) by combining porous layers (0.6 mm thick) with 0/90 degrees orientation in respect to the x-axis, in which each layer consist of parallel filaments separated by a specific gap, designed to be 0.65 mm, which is the pore size (PS) of the printed part; B) the 3D model in *STL* format file is exported to the slicing software (Cura from Ultimaker was used in this study*)* where it is sliced into horizontal layers with a defined thickness of 0.2 mm, resulting in a "3 slice per layer" approach. At the end of build step, a *gcode* file is created, which contains the path/coordinates than can be recognized by the printer to fabricate the 3D model; C) finally the gcode is sent to the printer which uses a temperature controlled nozzle (Ø0.4 mm), to extrude the PLA and deposit the semi-molten material onto a platform in a layer by layer process. The filament is moved by two rollers and acts as a piston to drive the semi-molten material.At the end of each finished layer, the platform is lowered and the next layer is deposited. The designed object is fabricated based solely on the precise deposition of thin layers that are made of parallel filaments deposited in X and Y directions. An approximately cube shaped porous structure was favoured to give a structure with equivalent accessibility from all three major axes. Parameters such as printing speed and printing temperature need to be carefully chosen to achieve a constant flow rate and consequently a constant filament width (FW) with a minimal fabrication time. After performing a preliminary study to assess the best combination of printing paremeters, the temperature and speed selected for printing the PLA porous bars were 210°C and 30 mm/s, respectively. Each sample took approximately 1 hour for being printed and 10 PLA scaffolds Ø10 mm discs were laser cut per printed bar.

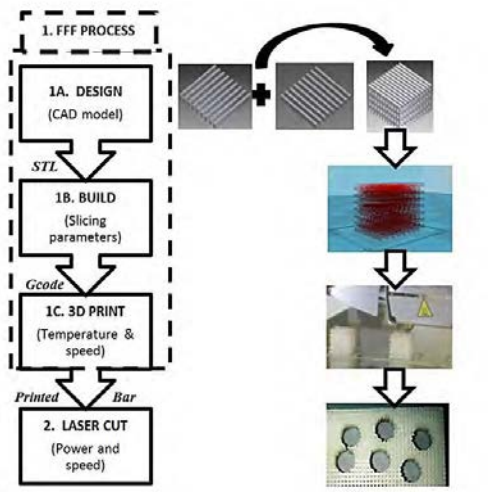

Fig.1.Schematic diagram describing PLA scaffold manufacturing route steps.

2.3. Material Characterisation

Due to the shear stresses and melting process that occur during printing and laser cutting processes, PLA degradation may occur during processing. Therefore PLA samples were extracted at the three PLA stages during scaffolds fabrication: 1) PLA filament, 2) Printed PLA and 3) Laser cut PLA and

their molecular weight (M_w) and thermal properties were investigated.

PLA samples molecular weight (M_w) distribution was determined with gel permeation chromatograph (GPC) equipped with a refractive index (RI) detector (Viscotek VE3580). The samples were dissolved in dimethylformamide and eluted in a series of configurations through a Styragel column refractor (Waters) at a flow rate of 0.6 mL min^{-1}. Polystyrene (PS) standards were used for determining the weight average molecular weight (M_w) and polydispersity index (PDI).

Thermal properties were determined by using a thermal analyser system, LABSYS Evo (Setaram). Samples of approximately 15-20 mg were loaded in aluminium pans and an empty aluminium pan with the same weight as the sample pan was used as reference. The samples were heated from 30ºC to 210ºC at a rate of 10 ºC /min, under a 40ml/min nitrogen atmosphere. Melting temperatures (T_m) were obtained at the peak of melting endotherms and glass transition temperatures (T_g) were acquired at the inflection point of the specific heat capacity.

2.4. Scaffold Morphological and Mechanical Testing

Morphological analysis of 3D structures was carried out with a Hitachi TM3030 Scanning Electron Microscope (SEM) to visualize and evaluate the architecture of the 3-D scaffolds and structural stability of the deposited filaments and layers.

As highlighted in Fig.2, from the top view images, pore size (PS) and filament width (FW) in the XY-axes were measured for the top layer, with this assumed to be indicative of pore sizes in the XY plane throughout the structure. The PS in XZ-axes or PS in the transversal direction was measured from the cross section images after cutting the sample with a scalpel. The PS and FW values were obtained by an average of five measurements and expressed as mean ± standard deviation (SD).

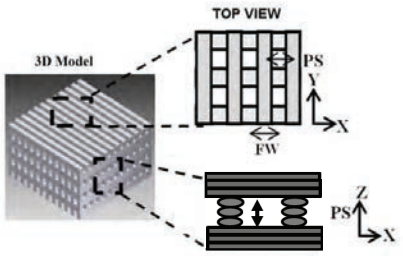

Fig.2. 3D model of porous structure with: Top view or XY axes and b) Cross section or XZ axes with a 3-layer approach. PS=pore size and FW= filament width.

The average scaffold porosity (P) was evaluated by the following Eq.2:

$$P = 1 - \rho_{scaffold} \,/\, \rho_{material}$$

Where $\rho\, material$ is the density of the material of which the scaffold is fabricated (PLA density= 1.24 g/cm^3) and $\rho\, scaffold$ is the apparent density of the scaffold measured by dividing the weight by the volume of the scaffold [6, 13].

Compression properties of porous PLA samples at different stages of scaffold fabrication were investigated, to assess the influence of processing on the mechanical behaviour. Compression samples (10x10x5mm) were prepared with 2 routes: 1) porous samples were 3D printed as explained in Fig.1 (FFF process) and 2) samples were laser cut from printed porous bars. A third group of PLA samples with a notionally fully dense structure were also printed and tested to obtain the material compressive properties rather than the apparent/structural compressive properties. All samples groups were tested under axial compression by loading at a speed of 1mm/s with a 5 kN load cell up to a strain level of approximately 60%. The compression modulus was calculated from the stress-strain curve as the slope of the initial linear portion of the curve. Compressive strength at yield was determined from the first point on the stress-strain curve at which an increase in strain was observed without an increase in stress. The compression modulus and yield strength for any given set of specimens were obtained by an average of five measurements and expressed as mean ± standard deviation (SD).

2.5. In vitro degradation study of PLA Scaffold

An *in vitro* degradation study of the porous PLA scaffolds (laser cut from printed bar) was carried out in PBS solution under pH 7.0 at 37ºC. Before immersion the samples were treated with air plasma by placing the scaffolds in a radiofrequency plasma chamber (PDC-32G, Harrick Plasma, USA) for 5 minutes with a medium inflow of air. Plasma cleaning was applied in order to obtain a more hydrophilic PLA surface, improving sample wetting upon immersion. Afterwards the samples were placed in 8ml weighing vials containing 4 ml PBS solution and were stored in an incubator at 37ºC for up to 8 weeks. At weekly intervals, the pH of the PBS solution was measured by pH meter and then replaced with fresh PBS. At approximately 2-week intervals, 3 samples of each scaffold type were removed from the vials for characterization. Characterisation of samples consisted in assessing the compressive properties with samples still in a wet state (with the procedure described previously in section 2.4). Due to the destructive nature of compression testing, another group of samples was vacuum dried for 48h and was characterized in terms of molecular weight (with the procedure described in section 2.3) and the sample dry weight was recorded with an analytical balance. All the characterisation results were presented as an average value of three measurements ± SD.

3. Results

3.1. Scaffold Fabrication

PLA scaffolds (Fig.3B) were successfully laser cut from a printed porous bar (Fig.3.A). As it can be seen in Fig.3.C, the laser cut sample presented a well-defined structure with open pores.

Fig.3. PLA scaffold fabrication process. A) Porous PLA printed bar with a zoom in (centre area) of top view (picture acquired with a stereomicroscope), B) Laser cut disc from A) and C) Laser cut disc surrounding edges.

3.2. Material Characterisation

Table 1 shows the results of DSC and GPC analysis. It can be observed that the M_w value of PLA decreased approximately 23% during FFF processing. The same trend was seen for the glass transition temperature that has decreased from 68ºC to 61ºC. The slightly decrease of both M_w and T_g after laser cutting was not significant.

Table 1. Values obtained from GPC and DSC analysis of PLA at different stages of processing.

	Mw	PDI	T_g	T_m
PLA. Filament	190 802	1.22	68	173
PLA. Printed. Bar	147 717	1.29	61	172
Laser.cut.PLA.scaffold	144 352	1.33	62	171

3.3. Morphological and Mechanical Behavior of PLA scaffold

SEM images of top view and cross section of laser cut PLA scaffold are presented in Fig.4. From both views, it is possible to observe a uniform pore distribution and well defined geometry. Also, in the cross section view, the scaffolds were characterised by a good interlayer adhesion and each layer is represented by 3 slices as defined during build step in the "3-slice per layer approach".

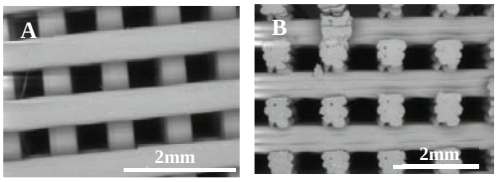

Fig.4. SEM images of laser cut PLA scaffold .A. Top view with 40X magnification and B. Middle cross-Section.

The measured values of PS in XY and XZ axes, FW and porosity % are summarized in Table 2.

Table2. Design parameters and values obtained after fabrication of PLA scaffold. The presented values are an average of 5 measurements with ± SD.

	Designed values (mm)	PLA scaffold (mm)
PS XY-plane	0.65	0.55 ± 0.02
PS XZ-plane	0.60	0.62 ± 0.01
FW	----	0.62 ± 0.01
Porosity	----	60

After printing, it was observed that the PS in the XY-axes was lower than the values set during design. Regarding the PS in the transversal direction, the values after printing were very close to the ones defined during design step.

The representative compression behaviour of the fabricated PLA scaffold is represented in Fig.5. Three stages were observed: 1) an initial linear elastic region followed by 2) a plateau of almost constant stress but increasing strain which is terminated by 3) an exponential increase in stress until the test ends.

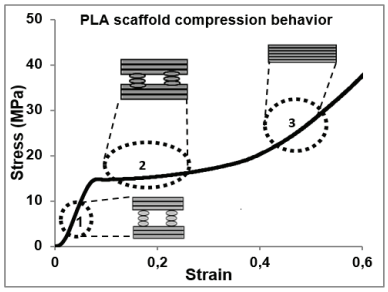

Fig.5. Stress-strain curve of PLA scaffold under compression loading. The stages are described schematically and explained in the discussion section.

The influence of laser cutting after printing on compression properties was investigated and the compressive modulus and stress at yield values obtained are summarised in Fig.6.A-B.

When comparing the influence of the structural properties in the compression behaviour, PLA samples with more void space (pores) presented lower values. Regarding the influence of the fabrication steps, after laser cutting, the PLA presented lower compressive properties with a decrease of ~27% in the compressive modulus and of ~35% in the stress at yield.

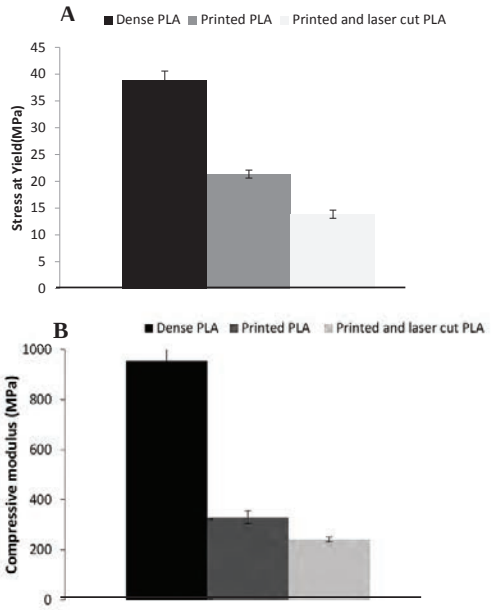

Fig.6. Compression properties of dense PLA and porous PLA printed and PLA laser cut from a printed bar (PLA scaffold). A. Stress at yield and B. Compressive modulus. Average values were plotted with ± SD.

3.4. In vitro degradation behavior

The pH variation during the *in vitro* degradation study is shown in Fig. 7. It has remained unchanged for up to 5 weeks around its initial value (pH~7). At week 6 the pH decreased to ~6.6 and it remained around this value until the end of 8 weeks study. The weight of PLA scaffolds remained also relatively constant throughout degradation of 8 weeks.

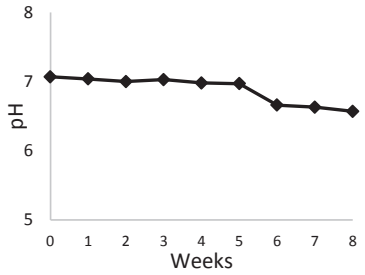

Fig.7. Change of pH of PBS solution used for *in vitro* degradation of porous PLA scaffolds.

The M_W and compressive properties evolution are illustrated in Fig.8.A-C. The compressive properties remained constant during 6 weeks. However at week 8 there was a significant increase in the compressive modulus from ~246 MPa to ~339 MPa. The molecular weight ($M_{W)}$ of PLA scaffold (Fig.8.C) did not present significant changes after 8 weeks of immersion in PBS.

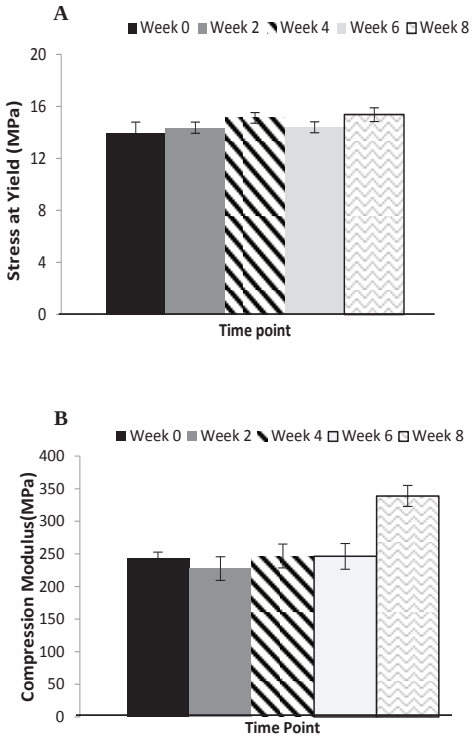

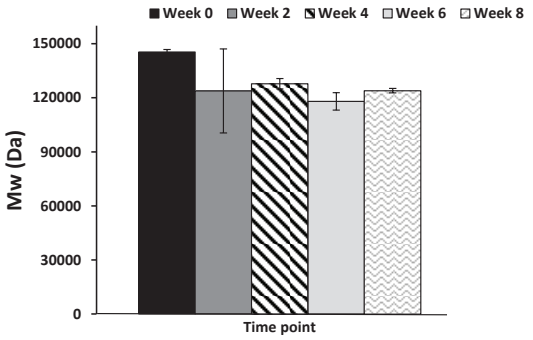

Fig.8. Results from in vitro degradation study of PLA scaffolds in PBS at 37°C. A) Stress at yield, B) Compression modulus and C) Average Molecular Weight (M_w). Average values of three replicates were plotted with ± SD.

4. Discussion

4.1. Material Degradation

A decrease in the glass transition temperature during PLA FFF fabrication was also observed by Dietmar et al. [12] can be attributed to degradation of the polymer during extrusion. The decreased molecular weight after processing could accelerate the *in vivo* degradation rate.

4.2. PLA scaffold Morphology and Mechanical Behaviour

Theoretically, the extruded FW should accord with the nozzle diameter (which was 0.4 mm for the FFF machine used in this work) or it should be slightly higher [14, 15]. For instance, Domingos et al. [15] reported FW values between ~0.30-0.43 mm when extruding a starch-based polymer (PCL) through a nozzle with a diameter of 0.3 mm, and varying the extrusion parameters. This is also in line with the findings of Hoque et al. [14], who have observed the same when extruding PLGA. The PS width in XY of ~0.55 mm vs the "as designed" 0.65 mm can be explained by the increased obtained FW value, as the sum of FD and PS will be constant.

The mechanical properties of 3D structures are an important feature when considering the scaffold application in bone tissue engineering. In this study, the PLA scaffold compression behavior was investigated and three regimes were observed as shown in Fig.5. Each regime corresponds to a specific mechanism of cell deformation as highlighted by the schematic designs of a porous structure next to each stage (Fig.5). In the first stage, the pore walls contribute to the resistance to the compressive load, which results in an elastic response to the load. In stage 2, the pores collapse by elastic buckling of the walls. At stage 3 the large increase in modulus is explained by the scaffolds now being effectively fully dense and further deformation compressing the material itself. The compression behaviour found in this work agrees with the behavior observed in other polymeric scaffold studies [16, 17].

According to the compression test results summarized in Fig.6, PLA laser cutting process led to a significant decrease in both stress at yield and compressive modulus. This behaviour could be caused mainly by differences in

morphology. The more open porosity means that there is some "redundant" material at the edges of the scaffold, which will not be load bearing. However, for a relatively small sacrifice in mechanical properties the higher open porosity could facilitate nutrients supply and waste removal and thus enhance vascularization and cell survival into the inner part of the scaffold.

The typical compressive strength of cancellous bone ranges from 2 to 12 MPa and its modulus is in the range of 0.1–5 GPa [18] , suggesting that the laser cut PLA scaffolds would be appropriate for this application.

4.3. In Vitro Degradation Behaviour

PLA scaffolds were immersed in PBS for 8 weeks and at week 6 a small pH decrease was observed (Fig.7). This could possibly be an indicator of polymer degradation as the by-products of PLA generate an acidic environment. However PLA scaffold weight, molecular weight and compressive property values did not decrease for 8 weeks, suggesting that the scaffold did not degrade significantly over the 8 week period. The increase in compressive modulus at week 8 is considered to be anomalous.

5. Conclusions

Additive manufacturing, in particular the FFF low-cost system used in this work, is suitable for fabricating 3-D porous structures with controlled pore sizes of greater than 500 μm and interconnected porosity.

Laser cutting of 3D printed PLA scaffolds did not affect the molecular weight and thermal properties of the polymer, but did slightly decrease in the mechanical properties by removing the capacity for some material within the structure to support load. However the PLA scaffolds compressive properties were found to be appropriate for trabecular bone applications.

After being immersed for 8 weeks in PBS at 37°C, laser cut PLA scaffolds did not shown any significant decrease in weight, compressive properties and molecular weight.

Overall the 2 step manufacturing route used in this work led to the fabrication of promising, mechanically stable scaffolds with well-defined and open architectures.

Acknowledgements

The research reported in this paper has been partly funded through MeDe Innovation (the EPSRC Centre for Innovative Manufacture in Medical Devices), the Arthritis Research UK Tissue Engineering Centre, the EC FP7 RESTORATION project (280575), and the Newcastle University EPSRC Doctoral Training Award.

References

1. Hao, L. and R. Harris, *Customised Implants for Bone Replacement and Growth*, in *Bio-Materials and Prototyping Applications in Medicine*, P. Bártolo and B. Bidanda, Editors. 2008, Springer US. p. 79-107.
2. Amini, A.R., C.T. Laurencin, and S.P. Nukavarapu, *Bone Tissue Engineering: Recent Advances and Challenges.* Critical reviews in biomedical engineering, 2012. **40**(5): p. 363-408.
3. Mollon, B., et al., *The clinical status of cartilage tissue regeneration.* Osteoarthritis and Cartilage, 2013. **21**(12): p. 1824-1833.
4. Schaefer, D., et al., *Tissue-engineered composites for the repair of large osteochondral defects.* Arthritis & Rheumatism, 2002. **46**(9): p. 2524-2534.
5. Grayson, W.L., et al., *Engineering custom-designed osteochondral tissue grafts.* Trends in Biotechnology, 2008. **26**(4): p. 181-189.
6. Karageorgiou, V. and D. Kaplan, *Porosity of 3D biomaterial scaffolds and osteogenesis.* Biomaterials, 2005. **26**(27): p. 5474-5491.
7. Jones, A.C., et al., *Analysis of 3D bone ingrowth into polymer scaffolds via micro-computed tomography imaging.* Biomaterials, 2004. **25**(20): p. 4947-54.
8. Murphy, C.M. and F.J. O'Brien, *Understanding the effect of mean pore size on cell activity in collagen-glycosaminoglycan scaffolds.* Cell Adhesion & Migration, 2010. **4**(3): p. 377-381.
9. Holmes, B., et al., *Development of Novel Three-Dimensional Printed Scaffolds for Osteochondral Regeneration.* Tissue Engineering Part A, 2014. **21**(1-2): p. 403-415.
10. Korpela, J., et al., *Biodegradable and bioactive porous scaffold structures prepared using fused deposition modeling.* J Biomed Mater Res B Appl Biomater, 2013. **101**(4): p. 610-9.
11. Frone, A.N., et al., *Morphology and thermal properties of PLA–cellulose nanofibers composites.* Carbohydrate Polymers, 2013. **91**(1): p. 377-384.
12. Dietmar, D., C.C. Sandra, and R. Dominik, *Suitability of PLA/TCP for fused deposition modeling.* Rapid Prototyping Journal, 2012. **18**(6): p. 500-507.
13. Tanaka, Y., et al., *The optimization of porous polymeric scaffolds for chondrocyte/atelocollagen based tissue-engineered cartilage.* Biomaterials, 2010. **31**(16): p. 4506-4516.
14. Hoque, M.E., et al., *Process Optimization to Improve the Processing of Poly (DL-lactide-co-glycolide) into 3D Tissue Engineering Scaffolds*, in *5th Kuala Lumpur International Conference on Biomedical Engineering 2011*, N. Osman, et al., Editors. 2011, Springer Berlin Heidelberg. p. 836-840.
15. Domingos, M., et al., *Effect of process parameters on the morphological and mechanical properties of 3D Bioextruded poly(ε - caprolactone) scaffolds.* Rapid Prototyping Journal, 2012. **18**(1): p. 56-67.
16. Ghassemieh, E., *Morphology and compression behaviour of biodegradable scaffolds produced by the sintering process.* Proc Inst Mech Eng H, 2008. **222**(8): p. 1247-62.
17. Hutmacher, D.W., et al., *Mechanical properties and cell cultural response of polycaprolactone scaffolds designed and fabricated via fused deposition modeling.* J Biomed Mater Res, 2001. **55**(2): p. 203-16.
18. Wu, S., et al., *Biomimetic porous scaffolds for bone tissue engineering.* Materials Science and Engineering: R: Reports, 2014. **80**(0): p. 1-36.